PHYSICAL REVIEW B VOLUME 27, NUMBER 11 1 JUNE 1983

Subharmonic energy-gap structure in superconducting constrictions

M. Octavio
Fundacion Instituto de Ingeniera, Apartado 1827, Caracas, Venezuela
and Division of Applied Sciences, Harvard University, Cambridge, Massachusetts 02138

M. Tinkham, G. E. Blonder,* and T. M. Klapwijk†
Physics Department, Harvard University, Cambridge, Massachusetts 02138
(Received 18 February 1983)

A Boltzmann-equation approach for the calculation of the I-V characteristics of superconducting constrictions is presented. This technique allows for the inclusion of normal scattering as well as Andreev reflection processes in the constriction. The computed I-V characteristics exhibit subharmonic gap structure which varies strongly with scattering strength and temperature. For even small scattering strengths, the structure is found to persist to $T=0$, and its temperature dependence agrees qualitatively with experimental observations. In the limit of zero scattering, the technique is shown to be equivalent to the trajectory technique of Klapwijk, Blonder, and Tinkham.

I. INTRODUCTION

While high-barrier tunneling devices have been well understood for a long time,[1] the understanding of continuous metallic weak links has evolved more slowly, due in part to the variety of experimental I-V characteristics which can be observed for the same device geometry. Two properties of the I-V characteristics which long lacked a satisfactory explanation are the subharmonic gap structure (SGS) and the excess current. These are usually observed in metallic weak links and very-low-barrier tunnel junctions, but not in high-barrier tunnel junctions. Here, the SGS refers to the series of peaks in the differential resistance dV/dI observed at submultiples of the gap voltage, $(2\Delta/e)/n$, where $n=1,2,3,\ldots$. The excess current, on the other hand, refers to the experimental observation that at voltages well *above* the gap, the current varies linearly with voltage but extrapolates to a positive (rather than zero) value at $V=0$. These phenomena have been studied experimentally by many workers in point contacts,[2–4] microbridges,[5–8] and shorted tunnel junctions.[9,10] Artemenko, Volkov, and Zaitsev[11] have shown that the excess current can be explained in terms of Andreev reflection. Using the Bogoliubov equations, Klapwijk, Blonder, and Tinkham[12] have recently shown that the subharmonic gap structure can be explained by the same mechanism. In this paper, we present a more complete version of this earlier work.

Earlier explanations for the SGS had been proposed in terms of multiparticle tunneling[13] and self-detection[14] of the Josephson radiation. Both of these mechanisms present difficulties. Multiparticle tunneling requires an n-particle tunneling process which occurs with a probability proportional to $|T|^{2n}$ where T is the tunneling matrix element. Given typical values of $|T|$, it is hard to reconcile observations of structure up to $n=12$ with the theoretical probability of the tunneling process; *very* low barriers would be required. The self-detection mechanism requires a separate explanation for the even and odd series in n, while experimental observations do not show significant differences in either the strength or the shape of the two series.

In their recent publication, Klapwijk, Blonder, and Tinkham (KBT) proposed[12] that the SGS can be explained in terms of multiple Andreev reflections[15] at the superconducting-normal interfaces of an *SNS* constriction, the thin-N region modeling the dissipative neck region across which the voltage is developed. What makes this model particularly appealing is that it provides a single explanation for both the even and odd series of the SGS, and, in junctions with dissimilar superconductors, predicts (for $\Delta_2 \gtrsim 2\Delta_1$) the existence of gap structure at $2\Delta_1/2n, \Delta_2$, and $(\Delta_2+\Delta_1)$, as observed experimentally. Furthermore, the application of similar concepts to the simpler *SN* constriction accounts rather well for the observed I-V characteristics of superconducting-normal point contacts[16,17] provided that nonzero probability for normal scattering at the interface is assumed. However, as a result of using the idealized zero-scattering limit, the KBT model for

the *SNS* contact yielded subgap structure which disappears as the temperature is reduced to $T=0$. As pointed out by KBT, it was expected that this deficiency would be cured by inclusion of a nonzero interfacial scattering probability, leading to a prediction of subharmonic gap structure at *all* temperatures. Unfortunately, the repeated branching within the trajectory technique of KBT makes it awkward to include normal scattering processes in that computational technique, so this expectation was not explicitly confirmed by KBT.

In this paper, a Boltzmann equation approach mentioned by KBT is presented which improves their earlier trajectory technique by making calculations explicitly self-consistent and allowing for the inclusion of scattering in the constriction in a computationally simpler manner. As noted by KBT, in the absence of scattering, this technique gives results identical to those that they obtained by the trajectory method. As shown in Sec. III, the effect of normal scattering is to increase the strength of the subharmonic gap structure and to preserve it even at the lowest temperatures. This leads to the curious conclusion that while the subharmonic gap structure is a consequence of *Andreev* reflection processes, it is the *normal* reflection processes which magnify the structure and allow for its observation at low temperatures. In addition to permitting inclusion of scattering effects, this technique also allows the direct calculation of the distribution function in the constriction.

Below, we begin in Sec. II by describing the Boltzmann-equation approach for an *SNS* junction with scattering at both interfaces and its relationship to the KBT approach. This is followed in Sec. III with the results of solving the equations for the nonequilibrium distribution functions and the *I-V* characteristics as a function of temperature and barrier strength. In Sec. IV we discuss our results and their applications, and finally, in Sec. V, we present our conclusions.

II. THE BOLTZMANN-EQUATION APPROACH

We assume the model of Fig. 1 in which a thin, fully normal metal extending from $x=0$ to L separates two superconducting films of the same material. At each *SN* interface we place a δ-function potential of strength $V(x)=H\delta(x)$, which simulates *elastic* scattering processes in the constriction, as well as any discontinuity in material parameters such as v_F (see Ref. 17). The three-dimensional contact is idealized as an insulating partition in which a small orifice of radius a communicates between the two superconducting banks. If the orifice size is assumed to be smaller than the coherence length, the gap rises on a scale comparable to a, and the potential drop will also occur over the same length scale. The mean free path l is also assumed to be larger than a. Within this model, the quasiparticles will gain energy on the scale of a, but will be diluted in the large three-dimensional banks, allowing us to describe the quasiparticles *incident* on the interfaces as thermally distributed quasiparticles with their distribution given by Fermi functions. The total current will depend on a weighted average of trajectories from all directions incident on the orifice. For simplicity, we have ignored this latter complication and have solved the Boltzmann equation within the one-dimensional model of Fig. 1.

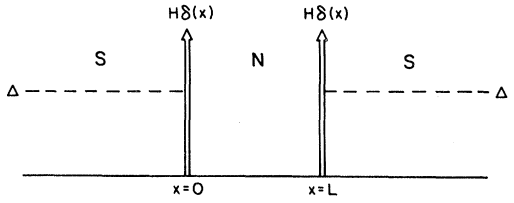

FIG. 1. One-dimensional *SNS* model for the superconducting constriction with δ-function potentials at the *SN* interfaces at $x=0$ and L, and $V=0$.

All elastic scattering events are assumed to occur at the *SN* interfaces, and no scattering events are assumed to occur in the normal region. This assumption will make the spatial dependence of the distribution function trivial, reflecting only the acceleration due to the applied voltage V. While the presence of the two δ functions may cause much of the potential drop to occur at the interfaces, we note that the energy gain upon one traversal between the two superconducting banks is eV, independent of the spatial distribution of the potential.

We work in the context of the generalized semiconductor model of Blonder *et al.*,[16] and sum all electron currents in the normal metal where electrons and holes are well defined. (In the banks, the quasiparticles are linear combinations of electrons and holes.) We separate the electrons into two subpopulations, based on direction of motion, described by two different nonequilibrium distribution functions $f_{\rightarrow}(E,x)$ and $f_{\leftarrow}(E,x)$, neither of which is assumed to be approximated by the equilibrium Fermi function within the normal region. Since all energies are measured with respect to the local chemical potential, electrons with energy E at $x=0$ have energy $E+eV$ when they arrive at the other superconductor at $x=L$. Similarly, electrons starting with energy E at $x=L$ will arrive at $x=0$ with energy $E-eV$. Thus we can write

$$f_{\rightleftarrows}(E,L)=f_{\rightleftarrows}(E-eV,0) \tag{1}$$

and describe the nonequilibrium distribution functions at both boundaries of the normal region by the pair of distribution functions $f_{\rightleftarrows}(E,0)$ together with Eq. (1). Next we need to relate $f_{\rightarrow}(E)$ and $f_{\leftarrow}(E)$ to the distribution functions in the superconducting regions. This can be accomplished by boundary conditions at the *SN* interfaces:

$$f_{\rightarrow}(E,0)=A(E)[1-f_{\leftarrow}(-E,0)] +B(E)f_{\leftarrow}(E,0)+T(E)f_0(E) \ , \tag{2a}$$

$$f_{\leftarrow}(E,L)=A(E)[1-f_{\rightarrow}(-E,L)] +B(E)f_{\rightarrow}(E,L)+T(E)f_0(E) \ . \tag{2b}$$

The coefficients $A(E)$, $B(E)$, and $T(E)$ describe Andreev reflection, normal reflection, and transmission as described in Ref. 16. Here we take $T(E)$ to be the total transmission coefficient with and without branch crossing; thus in the notation of Ref. 16, $T(E)=C(E)+D(E)$. Since the *incoming* population is taken to be in equilibrium because of coming from massive three-dimensional banks to an orifice small compared with the mean free path, we can simply use the Fermi function $f_0(E)$ in the terms describing the input of particles by transmission. The Andreev term is based on the fact that $1-f_{\leftarrow}(-E)$ is the probability that an incident hole with energy $-E$ will Andreev reflect and emerge as an electron with energy E. Since the conservation of probability requires that

$$A(E)+B(E)+T(E)=1 \tag{3}$$

only two of the coefficients in Eq. (3) can be varied independently. The coefficients $A(E)$, $B(E)$, and $T(E)$ depend on the strength of the normalized barrier $Z=H/\hbar v_F$, and thus the Boltzmann equation approach will allow us to calculate explicitly the more realistic case of finite scattering in the contact. It is important to note that the effect of the density of states in the superconductor is totally contained within the coefficients $A(E)$, $B(E)$, and $T(E)$, where E is measured relative to the electrochemical potential on the superconducting side of the interface.

We can now use Eq. (1) to rewrite Eq. (2b) by relating the distribution function at $x=L$ to that at $x=0$, leaving us with an equation at $x=0$:

$$f_{\leftarrow}(E-eV,0)=A(E)[1-f_{\rightarrow}(-E-eV,0)] +B(E)f_{\rightarrow}(E-eV,0)+T(E)f_0(E) \ . \tag{4}$$

Since the current will be the same at all positions in our one-dimensional model, it can be evaluated at $x=0$. Thus we are left with only the problem of evaluating $f_{\rightarrow}(E)$ at $x=0$, which allows us to drop the spatial index. If we then change variables by $E\rightarrow E+eV$, Eq. (4) is reduced to

$$f_{\leftarrow}(E)=A(E+eV)[1-f_{\rightarrow}(-E-2eV)] +B(E+eV)f_{\rightarrow}(E)+T(E+eV)f_0(E+eV) \tag{5}$$

This equation can now be used to eliminate $f_{\leftarrow}$ from Eq. (2a) leaving a single equation for the distribution function $f_{\rightarrow}$.

$$f_{\rightarrow}(E)=A(E)(1-\{A(-E+eV)[1-f_{\rightarrow}(E-2eV)]+B(-E+eV)f_{\rightarrow}(-E)+T(-E+eV)f_0(-E+eV)\}) +B(E)\{A(E+eV)[1-f_{\rightarrow}(-E-2eV)]+B(E+eV)f_{\rightarrow}(E)+T(E+eV)f_0(E+eV)\}+T(E)f_0(E) \tag{6}$$

This equation relates the distribution function of the subpopulation $f_{\rightarrow}(E)$ to those at $(E-2eV)$, $(-E-2eV)$, and $-E$ together with the external equilibrium source terms $f_0(E)$, $f_0(E+eV)$, and $f_0(-E+eV)$. The discrete system of equations given by Eq. (6) is infinite, but in practice it can be reduced to a finite set of equations since one expects $f_{\rightarrow}$ to approach 0 and 1 for $E\gg\Delta$ and $E\ll-\Delta$. Even when this truncation is made, the system remains rather large at small voltages, limiting the range of voltages for which a practical numerical solution can be achieved. Similarly the system grows as T approaches T_c. We have solved Eq. (6) by writing it in matrix form and solving it with a Gauss-Seidel algorithm, using the Fermi function as an initial guess. Once $f_{\rightarrow}(E)$ is obtained, Eq. (5) is used to obtain $f_{\leftarrow}(E)$.

As noted earlier, in our one-dimensional model we may calculate the current at any position; thus we only need to take the difference between $f_{\rightarrow}(E)$ and $f_{\leftarrow}(E)$ and integrate over E:

$$I=\mathscr{A}J =2N(0)ev_F\mathscr{A}\int_{-\infty}^{\infty}[f_{\rightarrow}(E)-f_{\leftarrow}(E)]dE \ , \tag{7}$$

where $\mathscr{A}$ is the effective cross-sectional area. In the

case of both sides of the interface being normal, $A=0$, $B=Z^2/(1+Z^2)$, and $T=1/(1+Z^2)$ and we can use Eqs. (5)–(7) to calculate the normal state resistance for the *SNS* model

$$I=\frac{2N(0)e^2v_F\mathscr{A}}{1+2Z^2}\equiv V/R_N \ . \tag{8}$$

Unlike the *NS* case,[16] which reduces exactly to the tunnel junction I-V curve in the high-barrier limit, here the I-V characteristics given by Eqs. (5)–(7) do *not* so reduce in that limit. The reason is that here we have modelled the constriction as having *two* separate δ-function potentials, one at each end of the normal region, which corresponds to a novel *SINIS* structure without elastic scattering in the normal region. For a realistic description of a dirty microbridge or the transition to the tunnel junction limit, a more general distribution of scattering potentials would be required.

It is instructive at this point to consider the relationship of the Boltzmann-equation approach to the earlier trajectory technique of KBT. In the absence of scattering, $B(E)=0$ and Eq. (6) can be written as

$$\begin{aligned} f_{\rightarrow}(E)=&A(E)T(E-eV)f_0(E-eV)\\ &+A(E)A(E-eV)f_{\rightarrow}(E-2eV)\\ &+T(E)f_0(E) \ . \end{aligned} \tag{9}$$

Similarly, by using (5) to eliminate $f_{\rightarrow}$ from (2a),

$$\begin{aligned} f_{\leftarrow}(E)=&A(E+eV)T(E+2eV)f_0(E+2eV)\\ &+A(E+eV)A(E+2eV)f_{\leftarrow}(E+2eV)\\ &+T(E+eV)f_0(E+eV) \ . \end{aligned} \tag{10}$$

Equations (9) and (10) represent the Boltzmann equation for the case of zero scattering and both distribution functions can be obtained iteratively since the two equations are now decoupled. In fact, the iteration corresponds to following the trajectory of an incoming electron through the two reflections needed for its reappearance as an electron. The general solution to Eq. (9) has the form

$$\begin{aligned} f_{\rightarrow}(E)=&T(E)f_0(E)+A(E)T(E-eV)f_0(E-eV)+A(E)A(E-eV)T(E-2eV)f_0(E-2eV)\\ &+A(E)A(E-eV)A(E-2eV)T(E-3eV)f_0(E-3eV)+\cdots \ . \end{aligned} \tag{11}$$

Similarly, for $f_{\leftarrow}(E)$, Eq. (10) has the solution:

$$\begin{aligned} f_{\leftarrow}(E)=&T(E+eV)f_0(E+eV)+A(E+eV)T(E+2eV)f_0(E+2eV)\\ &+A(E+eV)A(E+2eV)T(E+3eV)f_0(E+3eV)+\cdots \ . \end{aligned} \tag{12}$$

We can now use Eq. (7) to calculate the current. Since we integrate over all energies and since $A(E)\rightarrow 0$ for $E\gg 0$ and $E\ll -\Delta$, we can shift the origin of the energy in terms in (11) and (12) which contain Andreev reflection coefficients. In addition $T(E)=1-A(E)$, and the current can be written as

$$\begin{aligned} I=2N(0)ev_F\mathscr{A}\int_{-\infty}^{\infty}dE\{&[f_0(E)(1-A_0)(1+A_{-1}+A_{-1}A_{-2}+\cdots)]\\ &-[f_0(E-eV)(1-A_{-1})(1+A_0+A_0A_1+\cdots)]\} \ , \end{aligned} \tag{13}$$

where $A_n=A(E+neV)$. In this form Eq. (13) is exactly the same equation found by KBT using their different technique.

III. DISTRIBUTION FUNCTIONS AND I-V CHARACTERISTICS

One of the advantages of the Boltzmann-equation approach is that it allows for the direct calculation of the distribution functions in the constriction and thus gives some insight into their origin. Figure 2 shows the distribution functions for the two subpopulations $f_{\rightarrow}(E)$ and $f_{\leftarrow}(E)$ for the case of no scattering ($Z=0$), $T/T_c=0.95$, and bias voltage $eV=\Delta$. For energies outside the gap region, both distribution functions are smooth, while in the gap region, $f_{\rightarrow}(E)$ and $f_{\leftarrow}(E)$ consist of a sawtooth pattern with a periodicity of eV. It is this pattern which gives rise to the subharmonic gap structure as the bias voltage sweeps each discontinuity through the gap edge.

To understand the origin and periodicity of the structure in $f_{\rightarrow}(E)$ and $f_{\leftarrow}(E)$ it is useful to consider a schematic diagram such as that shown in Fig. 3, in addition to quantitative plots such as Fig. 2. Consider electrons incident from the left within the

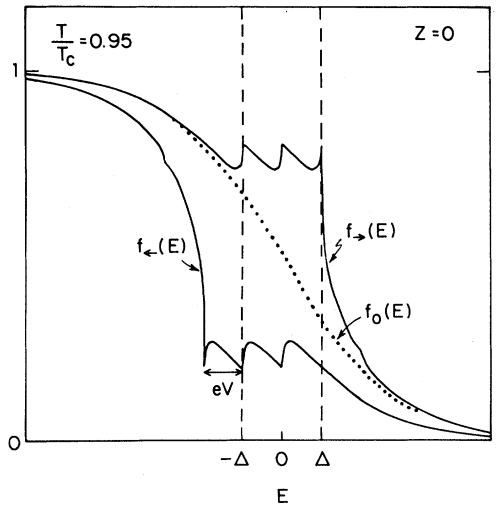

FIG. 2. Distribution functions $f_{\rightarrow}(E)$ and $f_{\leftarrow}(E)$ in the absence of scattering for $T/T_c=0.95$ and $eV=\Delta$. The equilibrium Fermi function $f_0(E)$ is shown (dotted line) for comparison.

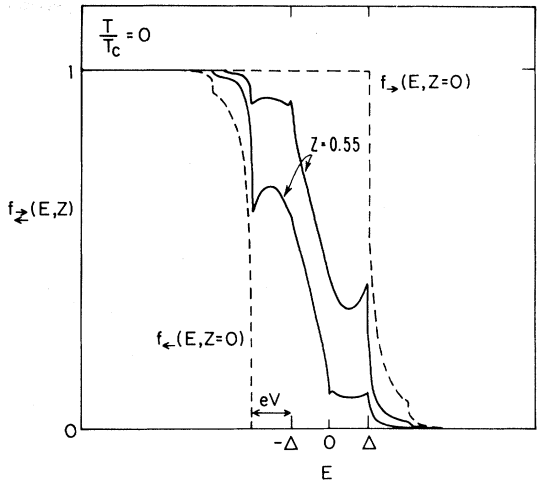

FIG. 4. Comparison of the distribution functions at $T=0$ for no scattering ($Z=0$, dashed lines) and finite scattering ($Z=0.55$, solid lines) for $eV=\Delta$. For $Z=1$ (not shown, to avoid confusion), $f_{\rightarrow}(E)$ and $f_{\leftarrow}(E)$ are still nearer each other, but retain sharp structure.

band of energies between $-\Delta$ and $-\Delta-eV$, where we indicate occupation numbers horizontally by a heavily shaded region. After one Andreev reflection indicated by the dashed trajectories, the band of electrons reappears as holes traveling to the left

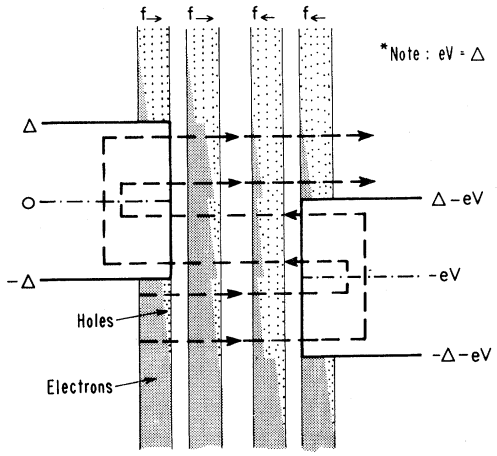

FIG. 3. Semiconductorlike picture showing the origin of the structure in the distribution function and its periodicity. The (schematic) distribution functions for electrons going in specific directions are shown heavily shaded while the complementary hole distributions are lightly shaded. The dashed lines trace representative trajectories through successive Andreev reflections. In making this figure, we have neglected scattering and also Andreev reflection outside the gap. The diagram represents the case $eV=\Delta\sim kT$, i.e., $T/T_c\sim 0.9$.

(represented by the lightly shaded area), which in turn Andreev reflect into electrons. The distribution function of these electrons corresponds to the initial distribution function shifted by $2eV$, the energy acquired by transversing the normal region twice. The intervening bands of electrons, of width eV, are filled by considering the electrons resulting from Andreev reflection of holes incident from the right, yielding the basic periodicity in eV. Note that in the figure we have for simplicity taken the special case $eV=\Delta$, assumed $Z=0$, and ignored Andreev reflection probabilities outside the gaps. If in constructing Fig. 3 we had not assumed a case for which $Z=0$, then not all of the incoming electrons in the appropriate energy band would be able to go through the first interface, nor would the transmitted fraction be completely reflected as holes at the second interface. The subharmonic gap structure originates from these bands in the distribution functions, as further reflections increase transfer to the opposite side, and the condition $V=2\Delta/ne$ corresponds to maximum electron transfer with given number of reflections.

Figure 4 shows the dramatic effect at $T=0$ including a finite scattering probability. For no scattering ($Z=0$), both $f_{\rightarrow}(E)$ and $f_{\leftarrow}(E)$ are essentially displaced Fermi (step) functions for $T=0$ except for structure for $E>\Delta$ in $f_{\rightarrow}(E)$ and $E<-(\Delta+eV)$ in $f_{\leftarrow}(E)$ related to the finite Andreev reflection probability above the gap. The effect of including a finite normal scattering probability (in this case, $Z=0.55$) at $T=0$ is to change the

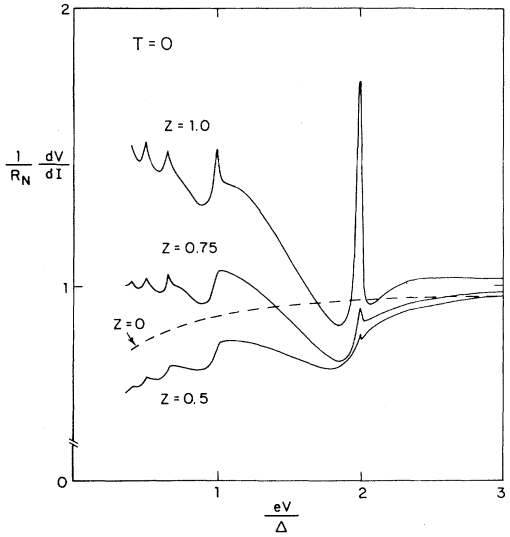

FIG. 5. Differential resistance dV/dI vs eV/Δ at $T=0$ as a function of barrier strength.

distribution functions to thermal-like functions for $T_{\text{eff}} \sim eV/k_B$, but with sharp structure with periodicity eV, as was shown in Fig. 2 for an actual temperature near T_c. Thus inclusion of normal scattering sharpens the structure in $f_{\rightleftarrows}(E)$ and, as shown below, in the I-V characteristics even at the lowest temperatures. [We have found it difficult to compute $f_{\rightleftarrows}(E)$ for $Z > 1$, as the structure in the distribution functions becomes so sharp that the numerical inversion of the system of equations given by Eq. (6) requires an increasingly larger number of iterations for convergence as Z is increased.]

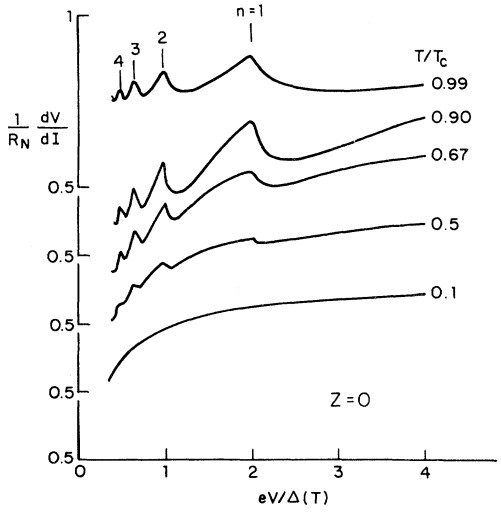

FIG. 6. Differential resistance dV/dI vs eV/Δ as a function of temperature in absence of scattering ($Z=0$).

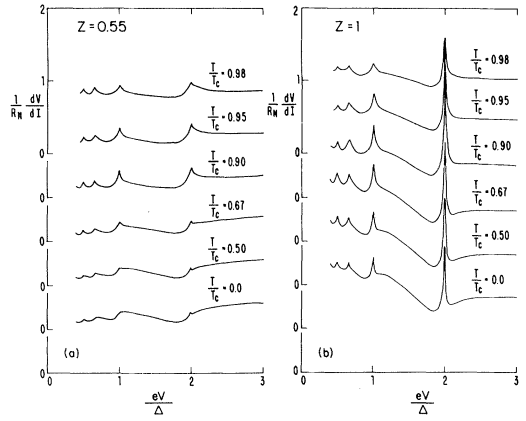

FIG. 7. Differential resistance dV/dI vs eV/Δ as a function of temperature in presence of scattering: (a) $Z=0.55$ and (b) $Z=1$.

Figure 5 shows the differential resistance dV/dI vs eV for $T=0$ as the barrier strength is changed from $Z=0$ to $Z=1$. The effect is quite dramatic, not only in sharpening the peaks at the gap and its subharmonics, but also in changing their overall shape. As noted earlier, for low voltages the system of equations given by Eq. (6) grows rapidly, making calculations in this regime extremely time consuming. Figures 6 and 7 show the differential resistance versus eV as a function of temperature for three values of the barrier strength $Z=0$, 0.55, and 1.0. The particular value $Z=0.55$ was chosen since in the SN constriction it was found to correspond closely to the excess current calculation of Artemenko, Volkov, and Zaitsev[11] for a dirty microconstriction. The value $Z=1$ corresponds to the case in which half of the incident electrons are scattered at each interface. In contrast to the case with no scattering ($Z=0$), the structure is present at all temperatures. The shape changes significantly as the temperature is lowered, with the changes being most dramatic for the 2Δ peak.

IV. APPLICATIONS AND DISCUSSION

While it was our original goal to provide a model which would allow quantitative comparison with experimental results, such comparison is difficult when dealing with real junctions. We believe that our model contains the essential physical processes leading to the subharmonic gap structure, namely, Andreev and normal reflection processes. The main approximation made has been the neglect of ac Josephson effect oscillations. While this could be

included by keeping track of phase dependent effects in calculating the transmission and reflection coefficients, the additional complexity would make explicit calculation of the I-V curves a formidable undertaking.

Most detailed measurements of the subharmonic gap structure have been made in superconducting microbridges, which typically do not satisfy the main assumptions of our model ($a < l, a < \xi$). As shown by Octavio *et al.*,[7] heating effects can significantly affect not only the shape but also the position of the subharmonic peaks, an effect which can be reduced significantly in high-resistance well-cooled microbridges. Such heating effects and also the effects of charge imbalance in the banks discussed by Peshkin and Buhrman[18] have not been included in our model. Furthermore, the I-V characteristics of most microbridges become hysteretic for low reduced temperatures, so that it is difficult to make comparisons with the whole range of variations predicted by our model.

Within the Boltzmann approach presented, it is possible to relax our assumption of a step-edge change in the gap. As pointed out by Blonder *et al.*,[16] for example, if the gap rises slowly with distance, the Andreev reflection coefficient in the absence of normal scattering jumps from one below the gap to essentially zero above the gap. This discontinuous jump in Andreev reflection probability would be expected to sharpen the structure in the distribution functions and hence of the subharmonic gap structure. We do not show the results of such calculations, however, since for $Z \neq 0$ they depend in detail on the spatial dependence of the gap and on the distribution of normal scattering centers.

While quantitative comparison is difficult, one can however compare the qualitative features predicted by our model with experimental results. At low temperatures, nonhysteretic data for the subharmonic gap structure are available only for point contact structures. Our model predicts that, depending on the amount of scattering, the 2Δ peak can be larger or smaller than the $n=2$ peak, a behavior found in Nb-Nb point contacts by Soerensen *et al.*[19] Furthermore, their data also exhibited the sharp drop in dV/dI between Δ/e and $2\Delta/e$ exhibited by our calculations.

In addition, our model predicts differences in the overall shape of the different peaks, which has also been observed experimentally.[5–7] The overall temperature dependence near T_c is also in qualitative agreement with those experimental results which show both the size and widths of the subharmonic peaks as the temperature is reduced. [Note that the voltage scale in Figs. 6 and 7 is normalized to $\Delta(T)$, which is temperature dependent; thus the widths of the peaks change in actual voltage units.]

As conceived, the model treats the superconducting constriction as an *SNS* device with all scattering assumed to occur at the *SN* interfaces. While this should be a reasonable approximation for metallic-like weak links, where the scattering is relatively weak, the model does not exhibit a proper crossover to tunnel-like behavior at high barrier strengths as it does for the single *SN* interface. Accordingly, we have restricted our computations to relatively weak scattering ($Z \leq 1$).

V. CONCLUSIONS

In this paper, we have presented an improved version of the KBT trajectory calculation[12] which first demonstrated that multiple Andreev reflections could provide a natural explanation for the subharmonic energy gap structure observed in the I-V curves of metallic weak links. This new version proceeds by solving the Boltzmann equation for the electron populations in the quasinormal constriction, taking account of normal as well as Andreev reflections at the interfaces with the superconducting banks, in addition to electrons transmitted to and from the banks. In the absence of normal scattering (reflection) processes, our results exactly reproduce the results of KBT, but in the presence of normal scattering, new features appear. In particular, the subharmonic gap structure is found to persist to $T=0$, whereas it was found to fade out for $T \ll T_c$ in the absence of scattering. In addition, there are more subtle differences in the sharpness and shape of the structure.

Although the range of types of SGS observed experimentally is almost endless, making a detailed comparison of doubtful significance, there is a reasonable degree of qualitative agreement between our predictions and the data. Moreover, it should be noted that our idealized model ignores not only the Josephson effect, but also all nonequilibrium effects in the banks, such as heating and charge imbalance, which are undoubtedly important in many practical geometries. Accordingly, we have not attempted any detailed fits to published data, but new data, taken under conditions chosen to minimize nonequilibrium effects, could provide a valuable comparison with our predictions.

ACKNOWLEDGMENTS

One of us (M.O.) would like to thank G. Fernandez and K. Octavio for useful suggestions and to thank the U. S. Office of Naval Research and the Venezuelan Consejo Nacional de Investigaciones

Cientificas y Tecnologicas for research support. One of us (G.E.B.) was supported by an IBM fellowship during part of this work. One of us (T.M.K.) would like to thank the Nederlandse Organisatie voor Zuiver Wetenschappelijk Onderzoek for a grant. The work at Harvard was supported in part by NSF Grant No. DMR-79-04155 and by the Joint Services Electronics Program.

---

*Present address: Bell Laboratories, Murray Hill, NJ 07974.

†Permanent address: Laboratorium voor Technische Natuurkunde, Technische Hogeschool Delft, Delft, The Netherlands.

[1]See, for example, W. L. McMillan and and J. M. Rowell, in *Superconductivity,* edited by R. D. Parks (Dekker, New York, 1969), Vol. 1, p. 561.

[2]L. J. Barnes, Phys. Rev. 184, 434 (1969).

[3]D. A. Weitz, Harvard University, Division of Applied Sciences, Report No. 14 (unpublished).

[4]Yu. Ya. Divin and F. Ya. Nad', Zh. Eksp. Teor. Fiz. Pis'ma Red. 29, 567 (1979) [JETP Lett. 29, 516 (1979)].

[5]P. E. Gregers-Hansen, E. Hendricks, M. T. Levinsen, and G. R. Pickett, Phys. Rev. Lett. 31, 524 (1973).

[6]I. K. Yanson, Fiz. Nizkikh Temp. 1, 141 (1975) [Sov. J. Low. Temp. Phys. 1, 67 (1975)].

[7]M. Octavio, W. J. Skocpol, and M. Tinkham, IEEE Trans. Magn. MAG-13, 739 (1977).

[8]M. Octavio, Harvard University, Division of Applied Sciences, Report No. 13 (unpublished).

[9]J. M. Rowell and W. L. Feldmann, Phys. Rev. 172, 393 (1968).

[10]M. Octavio, A. Sa-Neto, and R. C. Callarotti, Physica 108B + C, 973 (1981).

[11]S. N. Artemenko, A. F. Volkov, and A. V. Zaitsev, Zh. Eksp. Teor. Fiz. Pis'ma Red. 28, 637 (1978) [JETP Lett. 28, 589 (1978)]; also, Zh. Eksp. Teor. Fiz. 76, 1816 (1979) [Sov. Phys.—JETP 49, 924 (1979)].

[12]T. M. Klapwijk, G. E. Blonder, and M. Tinkham, Physica 109-110B + C, 1657 (1982).

[13]J. R. Schrieffer and J. W. Wilkins, Phys. Rev. Lett. 10, 17 (1963).

[14]N. R. Werthamer, Phys. Rev. 147, 255 (1966).

[15]A. F. Andreev, Zh. Eksp. Teor. Fiz. 46, 1823 (1964) [Sov. Phys.—JETP 19, 1228 (1964)].

[16]G. E. Blonder, M. Tinkham, and T. M. Klapwijk, Phys. Rev. B 25, 4515 (1982).

[17]G. E. Blonder and M. Tinkham, Phys. Rev. B 27, 112 (1983).

[18]M. Peshkin and R. A. Buhrman, Phys. Rev. B (in press).

[19]O. Hoffman Soerensen, B. Kofoed, N. F. Pedersen, and S. Shapiro, Phys. Rev. B 9, 3746 (1974).